Synthesis, characterization and reactivity of PCN pincer nickel complexes

Abdelrazek H. Mousa [a], Jesper Bendix [b] and Ola F. Wendt [a]*

[a] *Centre for Analysis and Synthesis, Department of Chemistry, Lund University, P. O. Box 124, S-221 00 Lund, Sweden.*

[b] *Department of Chemistry, University of Copenhagen, Universitetsparken 5, DK-2100 Copenhagen , Denmark.*

CONTENTS

Table S1. Crystallographic data and structure refinement details for complexes **1-3**

	1	**2**	**3**
Empirical formula	$C_{18}H_{31}ClNNiP$	$C_{18}H_{33}Cl_3NNiP$	$C_{18}H_{31}BrNNiP$
Formula weight	386.57	459.48	431.03
Temperature/K	293(2)	293(2)	293(2)
Crystal system	Monoclinic	Monoclinic	Monoclinic
Space group	$P2_1/c$	$P2_1/n$	$P2_1/c$
a/Å	13.8841(9)	11.4619(2)	14.0308(4)
b/Å	11.7651(5)	14.0718(2)	11.9479(2)
c/Å	11.8029(7)	14.2420(2)	11.8830(3)
α/°	90	90	90
β/°	95.208(5)	102.135(2)	95.187(2)
γ/°	90	90	90
Volume/Å^3	1920.02(19)	2245.76(6)	1983.89(8)
Z	4	4	4
ϱ_{calc}g/cm^3	1.337	1.359	1.443
μ/mm^{-1}	1.230	1.293	3.070
F(000)	824.0	968.0	896.0
2Θ range for data collection/°	5.552 to 58.696	5.79 to 57.206	4.844 to 57.564
Index ranges	$-18 \le h \le 18$ $-15 \le k \le 15$ $-16 \le l \le 16$	$-15 \le h \le 14$ $-18 \le k \le 18$ $-18 \le l \le 18$	$-18 \le h \le 18$ $-15 \le k \le 15$ $-15 \le l \le 15$
Reflections collected	19617	25039	22173
Independent reflections	4754 [R_{int} = 0.1034 R_{sigma} = 0.0935]	5321 [R_{int} = 0.0343 R_{sigma} = 0.0302]	4758 [R_{int} = 0.0338 R_{sigma} = 0.0249]
Data/restraints/parameters	4754/0/207	5321/0/225	4758/0/207
Goodness-of-fit on F^2	1.017	1.038	1.026
Final R indexes [I>=2σ (I)]	R_1 = 0.0574 wR_2 = 0.1035	R_1 = 0.0359 wR_2 = 0.0759	R_1 = 0.0288 wR_2 = 0.0657
Final R indexes [all data]	R_1 = 0.1037 wR_2 = 0.1272	R_1 = 0.0583 wR_2 = 0.0848	R_1 = 0.0388 wR_2 = 0.0697
Largest diff. peak/hole / e Å^{-3}	0.58/-0.56	0.49/-0.31	0.57/-0.38
CCDC	1842121	1842126	1842122

Table S2. Crystallographic data and structure refinement details for complexes **4-6**

	4	**5**	**6**
Empirical formula	$C_{18}H_{31}Cl_2NNiP$	$C_{18}H_{31}Br_2NNiP$	$C_{18}H_{31}N_2NiO_3P$
Formula weight	422.02	510.94	413.13
Temperature/K	293(2)	293(2)	293(2)
Crystal system	Monoclinic	Orthorhombic	Monoclinic
Space group	$P2_1/c$	Pbca	$P2_1/n$
a/Å	16.8982(9)	8.6035(11)	9.2618(11)
b/Å	8.5389(4)	15.379(2)	15.4127(14)
c/Å	14.8122(6)	32.418(4)	14.8841(17)
α/°	90	90	90
β/°	104.453(5)	90	94.817(10)
γ/°	90	90	90
Volume/Å^3	2069.64(17)	4289.5(8)	2117.2(4)
Z	4	8	4
ϱ_{calc}g/cm^3	1.354	1.582	1.296
μ/mm^{-1}	1.272	4.705	1.009
F(000)	892.0	2072.0	880.0
2Θ range for data collection/°	6.37 to 57.614	5.98 to 57.632	4.998 to 57.774
Index ranges	$-22 \le h \le 22$ $-10 \le k \le 11$ $-19 \le l \le 19$	$-11 \le h \le 11$ $-19 \le k \le 19$ $-42 \le l \le 40$	$-12 \le h \le 12$ $-20 \le k \le 19$ $-19 \le l \le 19$
Reflections collected	23478	24699	23819
Independent reflections	4967 [R_{int} = 0.0532 R_{sigma} = 0.0647]	5116[R_{int} = 0.0630 R_{sigma} = 0.0634]	5108 [R_{int} = 0.0977 R_{sigma} = 0.0596]
Data/restraints/parameters	4967/0/248	5116/0/216	5108/0/228
Goodness-of-fit on F^2	0.906	1.060	1.037
Final R indexes [I>=2σ (I)]	R_1 = 0.0425 wR_2 = 0.0903	R_1 = 0.0629 wR_2 = 0.1000	R_1 = 0.0449 wR_2 = 0.1018
Final R indexes [all data]	R_1 = 0.0787 wR_2 = 0.1087	R_1 = 0.1255 wR_2 = 0.1213	R_1 = 0.0664 wR_2 = 0.1151
Largest diff. peak/hole / e Å^{-3}	0.35/-0.29	0.90/-1.04	0.33/-0.36
CCDC	1842124	1842118	1842123

Table S3. Crystallographic data and structure refinement details for complexes **10,13-15**

	10	**13**	**14**	**15**
Empirical formula	$C_{37}H_{62}N_2Ni_2O_3P_2$	$C_{19}H_{34}NNiP$	$C_{24}H_{36}NNiP$	$C_{27}H_{38}NNiP$
Formula weight	762.24	366.15	428.22	466.26
Temperature/K	293(2)	293(2)	293(2)	293(2)
Crystal system	Monoclinic	Monoclinic	Triclinic	Monoclinic
Space group	$P2_1/c$	$P2_1/c$	P-1	C2/c
a/Å	12.4154(4)	13.8749(3)	7.6857(4)	25.302(3)
b/Å	20.3080(7)	11.8415(3)	9.9501(8)	15.9046(5)
c/Å	19.2503(9)	11.8811(3)	16.4908(13)	20.526(3)
α/°	90	90	84.626(7)	90
β/°	107.527(4)	94.626(2)	77.746(6)	141.46(3)
γ/°	90	90	70.306(7)	90
Volume/Å^3	4628.3(3)	1945.70(8)	1159.95(15)	5147(2)
Z	4	4	2	8
ϱ_{calc}g/cm^3	1.094	1.250	1.226	1.204
μ/mm^{-1}	0.913	1.077	0.913	0.829
F(000)	1632.0	792.0	460.0	2000.0
2Θ range for data collection/°	6.122 to 58.636	5.83 to 57.648	5.738 to 58.264	5.122 to 57.65
Index ranges	$-17 \le h \le 16$ $-27 \le k \le 27$ $-25 \le l \le 25$	$-18 \le h \le 18$ $-16 \le k \le 14$ $-15 \le l \le 16$	$-10 \le h \le 10$ $-13 \le k \le 13$ $-21 \le l \le 22$	$-34 \le h \le 33$ $-21 \le k \le 20$ $-27 \le l \le 27$
Reflections collected	51734	22308	25388	55093
Independent reflections	11437 [R_{int} = 0.0635; R_{sigma} = 0.0731]	4611 [R_{int} = 0.0420; R_{sigma} = 0.0381]	5724 [R_{int} = 0.0780; R_{sigma} = 0.0623]	6339 [R_{int} = 0.1012; R_{sigma} = 0.0552]
Data/restraints/parameters	11437/0/431	4611/0/208	5724/93/283	6339/0/280
Goodness-of-fit on F^2	0.991	1.037	1.117	1.047
Final R indexes [I>=2σ (I)]	R_1 = 0.0516, wR_2 = 0.1027	R_1 = 0.0370, wR_2 = 0.0728	R_1 = 0.0820 wR_2 = 0.2304	R_1 = 0.0567 wR_2 = 0.1311
Final R indexes [all data]	R_1 = 0.1049 wR_2 = 0.1215	R_1 = 0.0591 wR_2 = 0.0807	R_1 = 0.1090 wR_2 = 0.2501	R_1 = 0.0924 wR_2 = 0.1501
Largest diff. peak/hole / e Å^{-3}	0.33/-0.26	0.29/-0.27	1.22/-0.63	0.69/-0.41
CCDC	1842125	1842120	1842119	1842127

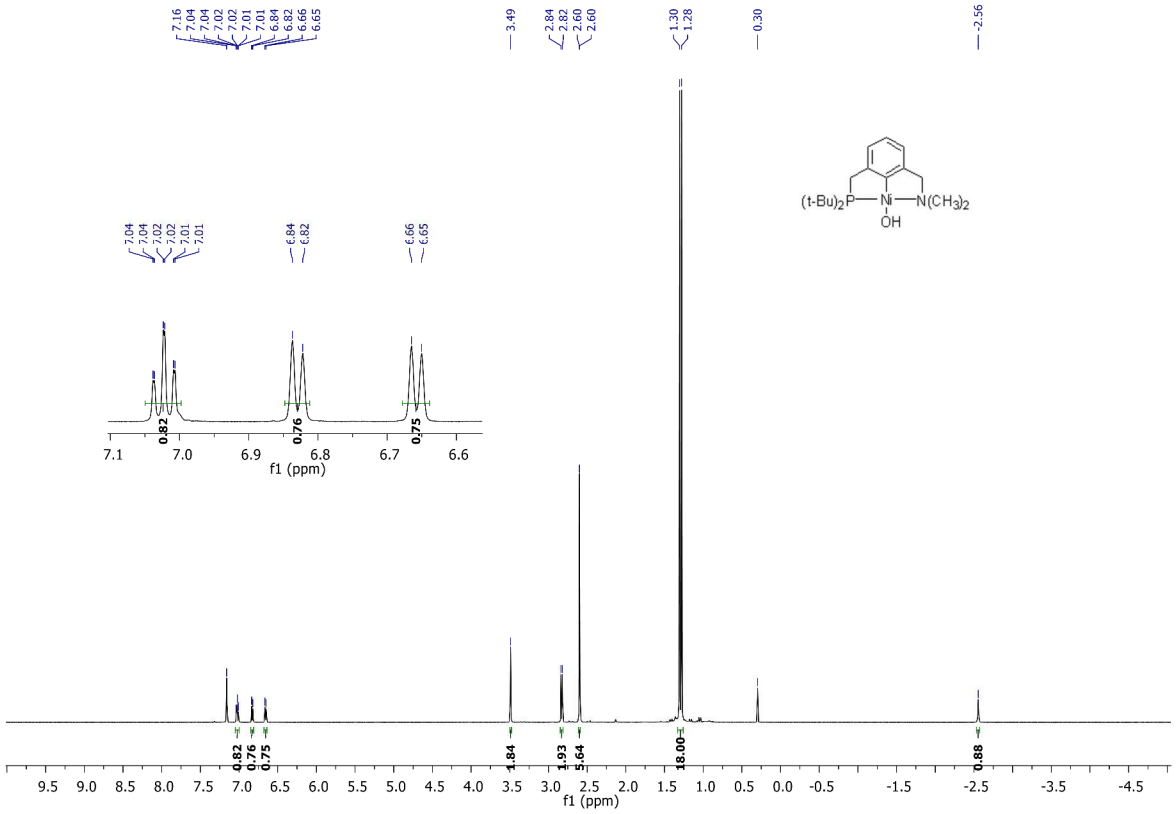

Figure S1.[1]H NMR spectrum (500 MHz, C_6D_6) of (PCN^{Me})Ni-OH(**8**) including traces of silicon grease.

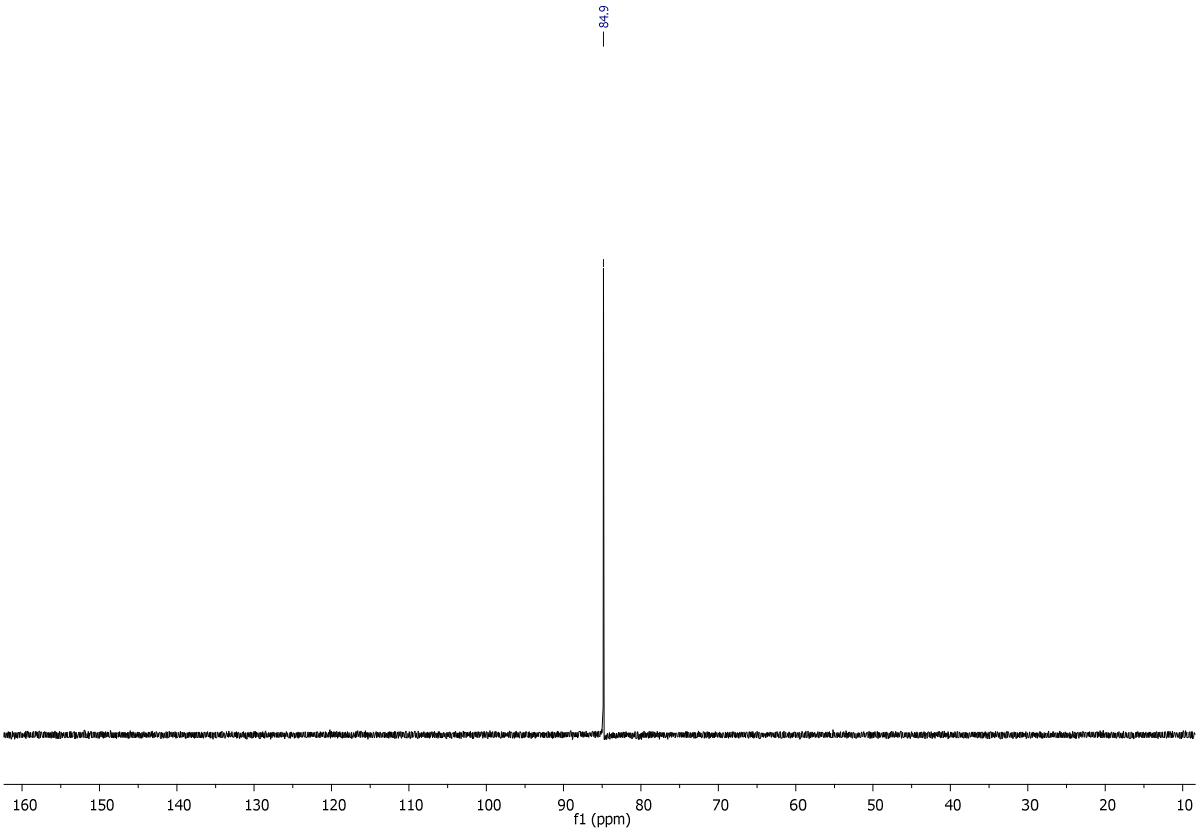

Figure S2.[31]P{[1]H} NMR spectrum (202 MHz, C_6D_6) of (PCN^{Me})Ni-OH(**8**).

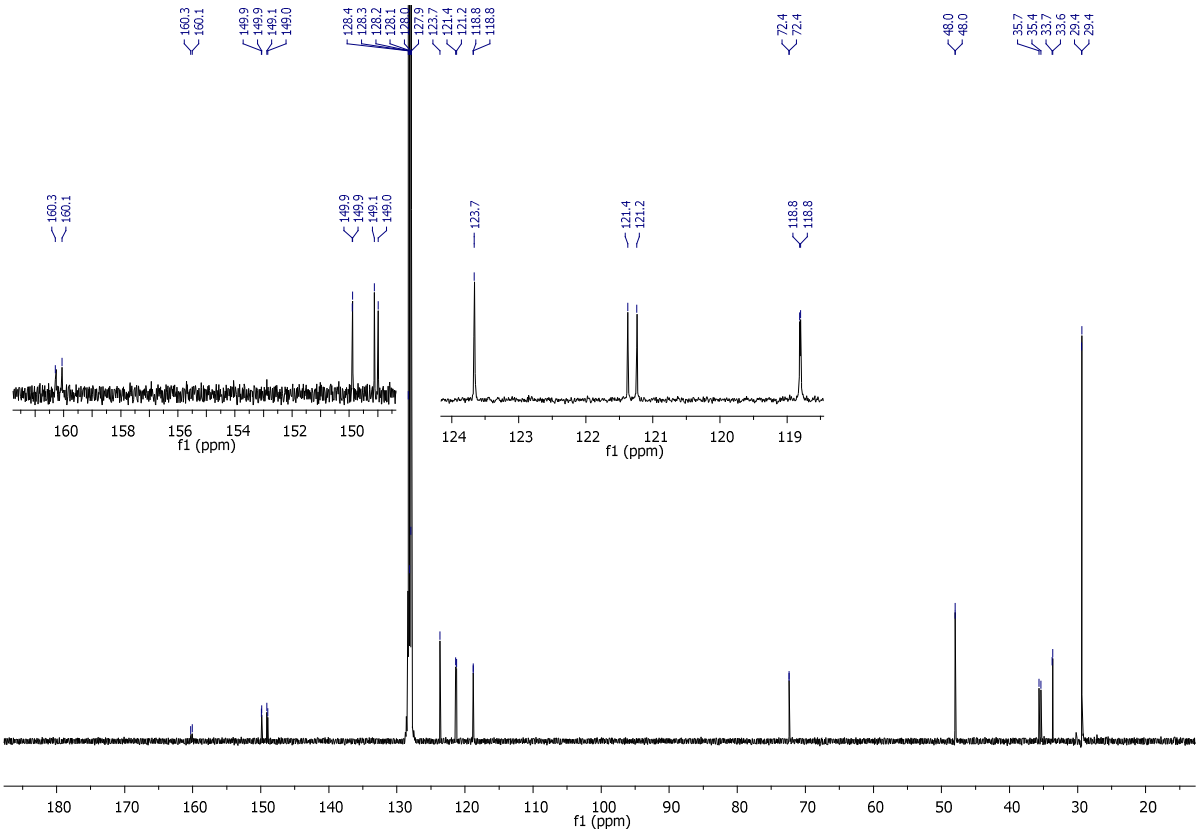

Figure S3.$^{13}C\{^{1}H\}$NMR spectrum (126 MHz, C_6D_6) of (PCN^{Me})Ni-OH(**8**).

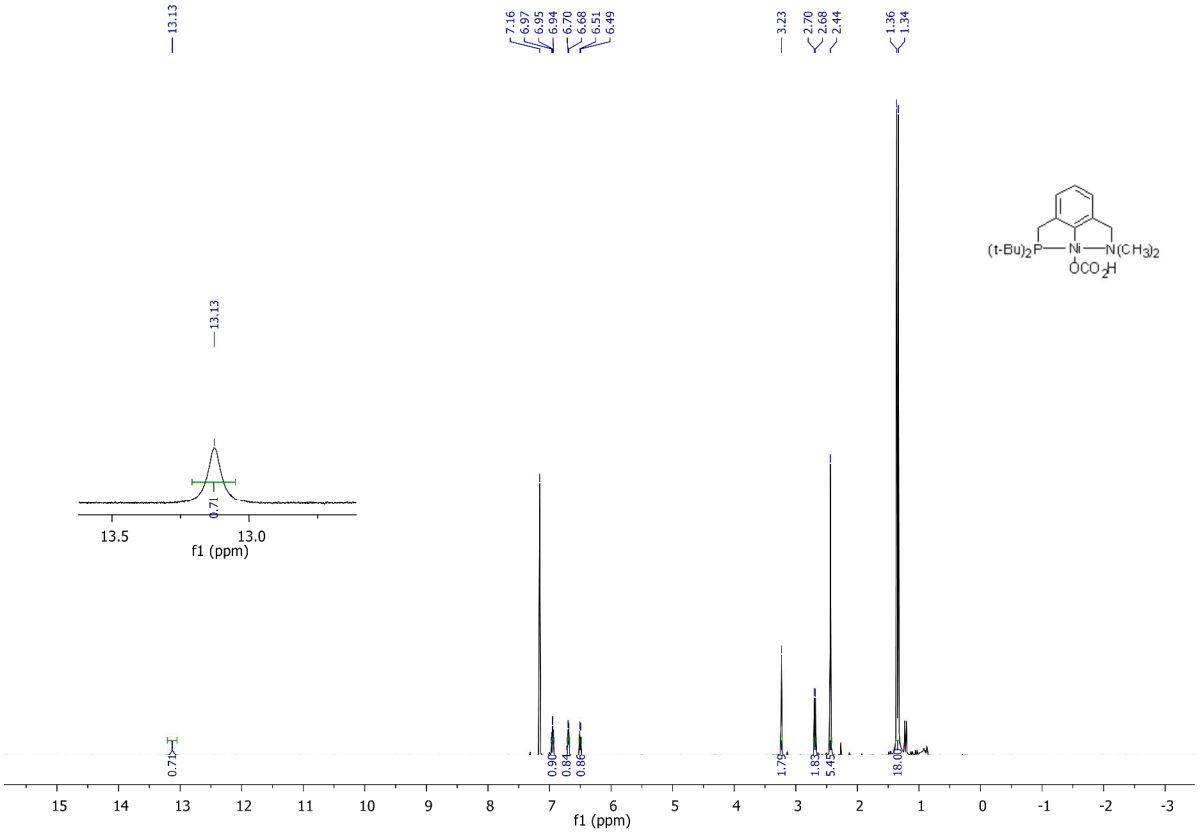

Figure S4.^{1}H NMR spectrum (500 MHz, C_6D_6) of (PCN^{Me})Ni-OCO_2H(**9**)

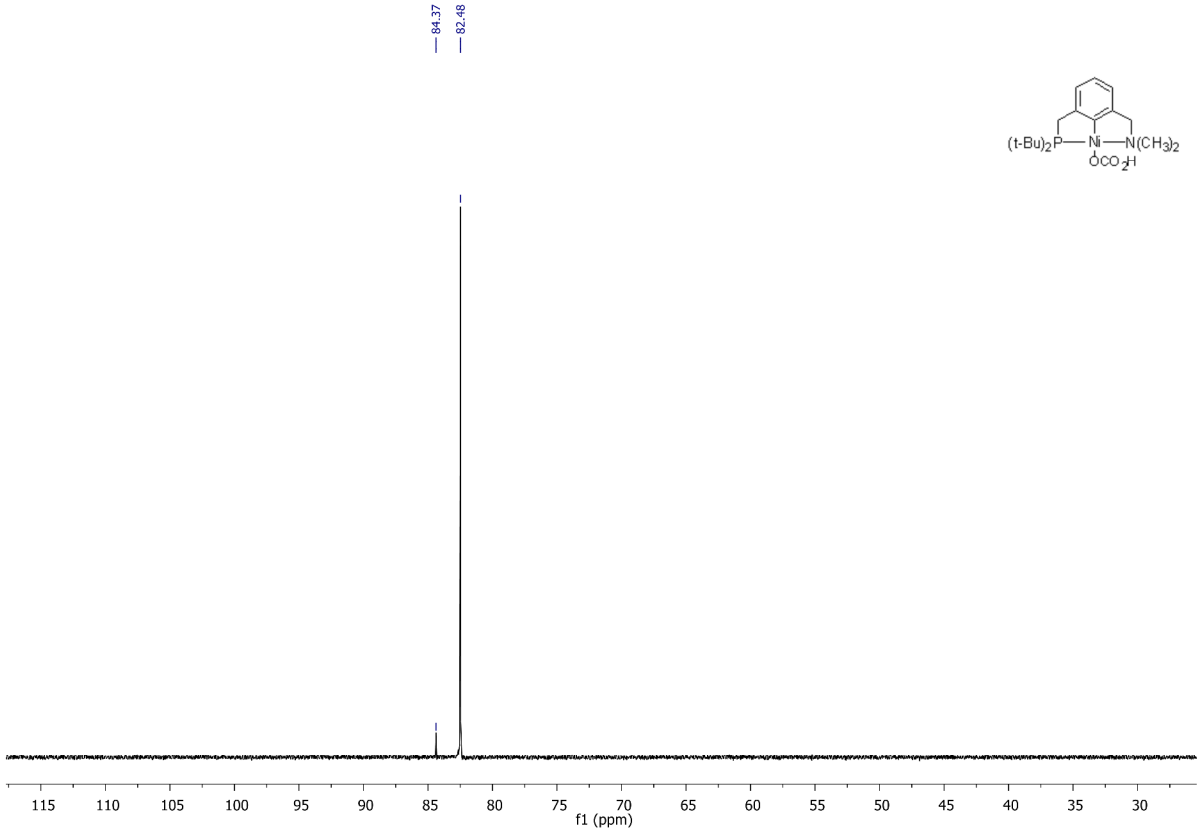

Figure S5.$^{31}P\{^{1}H\}$ NMR spectrum (202 MHz, C_6D_6) of (PCN^{Me})Ni-OCO_2H(**9**)

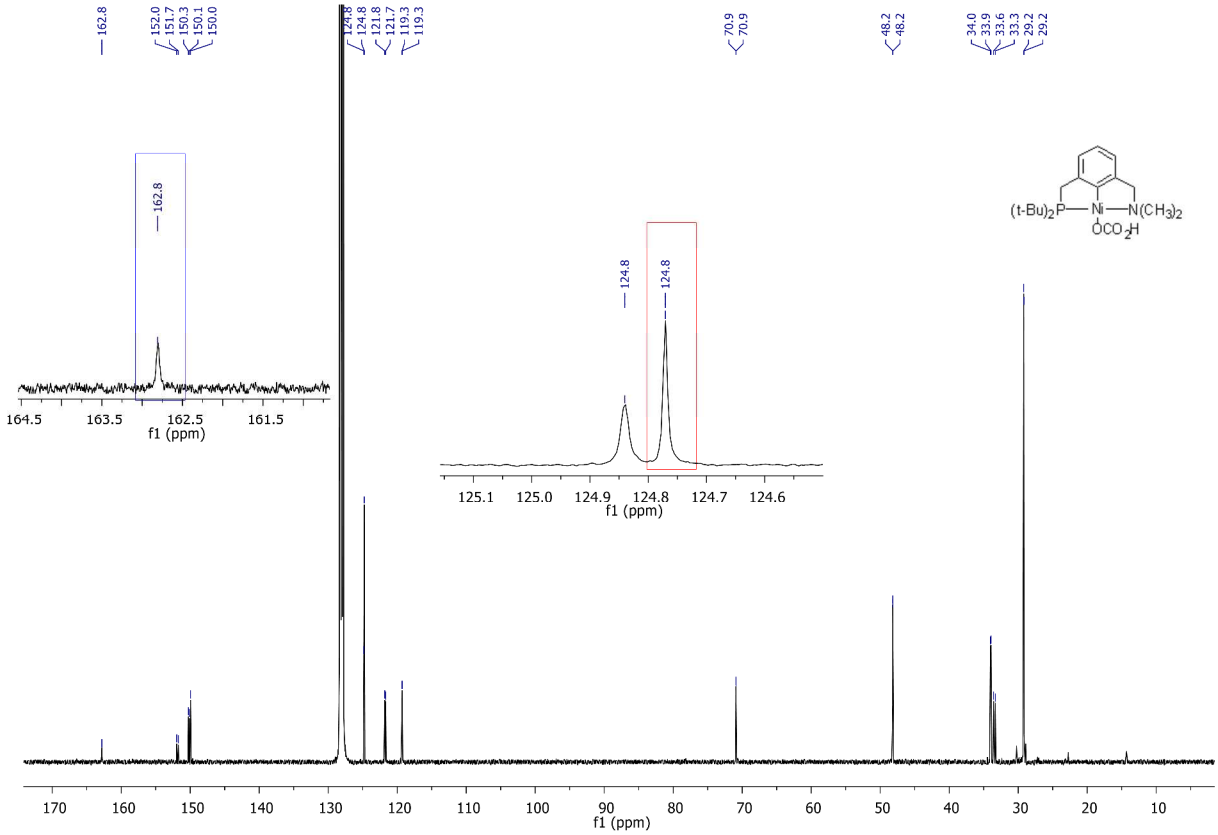

Figure S6.$^{13}C\{^{1}H\}$ NMR spectrum (126 MHz, C_6D_6) of (PCN^{Me})Ni-OCO_2H(**9**)

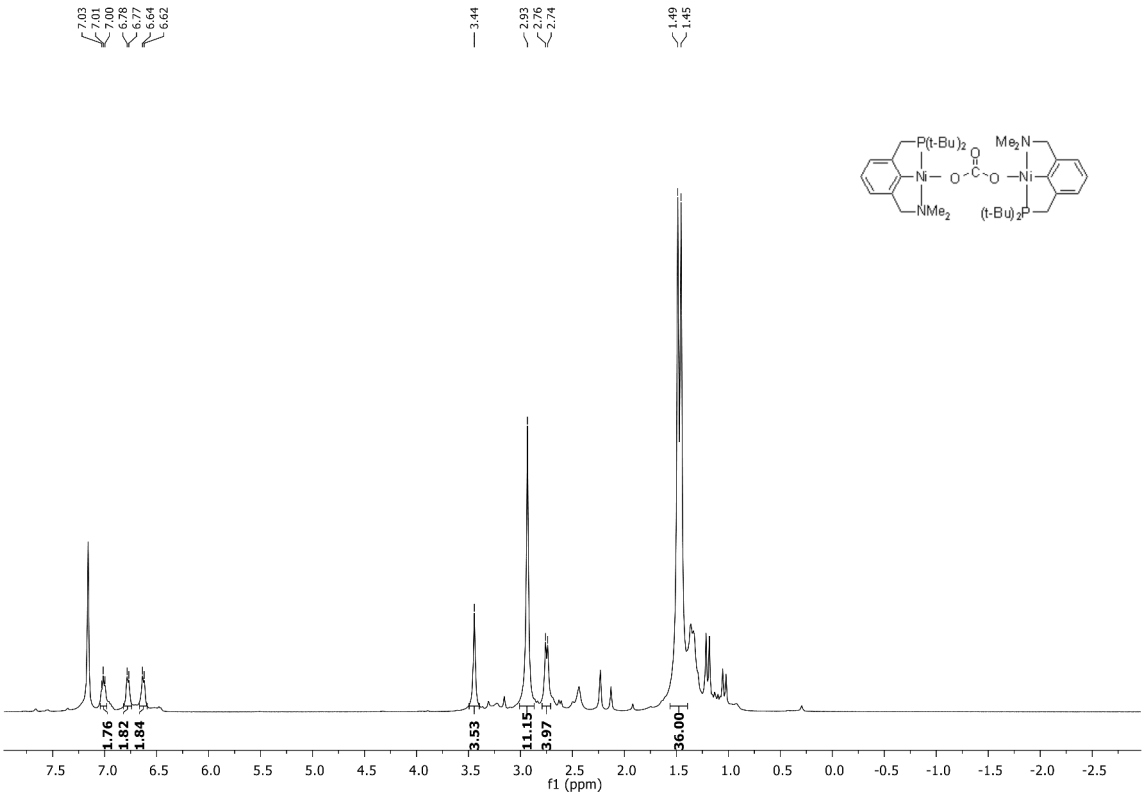

Figure S7.[1]H NMR spectrum (500 MHz, C_6D_6) of {(PCN^{Me})Ni}$_2$(μ-CO_3)(**10**)

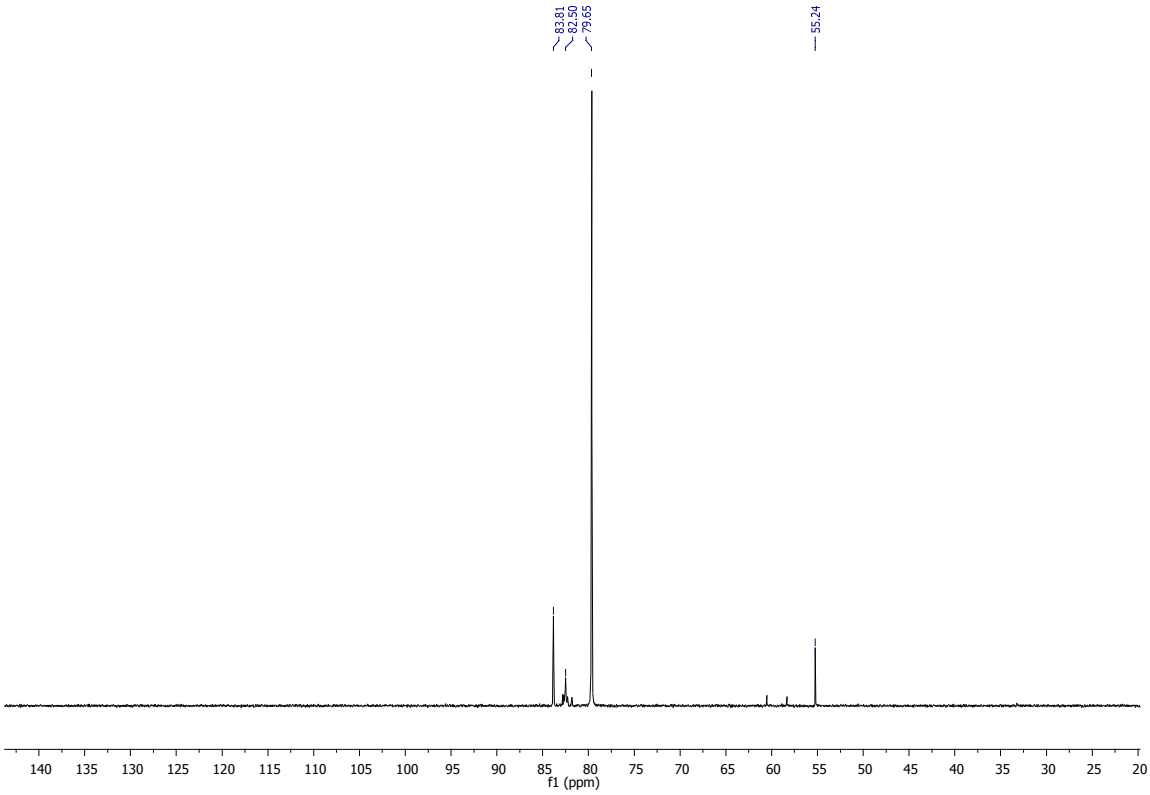

Figure S8. $^{31}P\{^1H\}$ NMR spectrum (202 MHz, C_6D_6) of {(PCN^{Me})Ni}$_2$(μ-CO_3)(**10**)

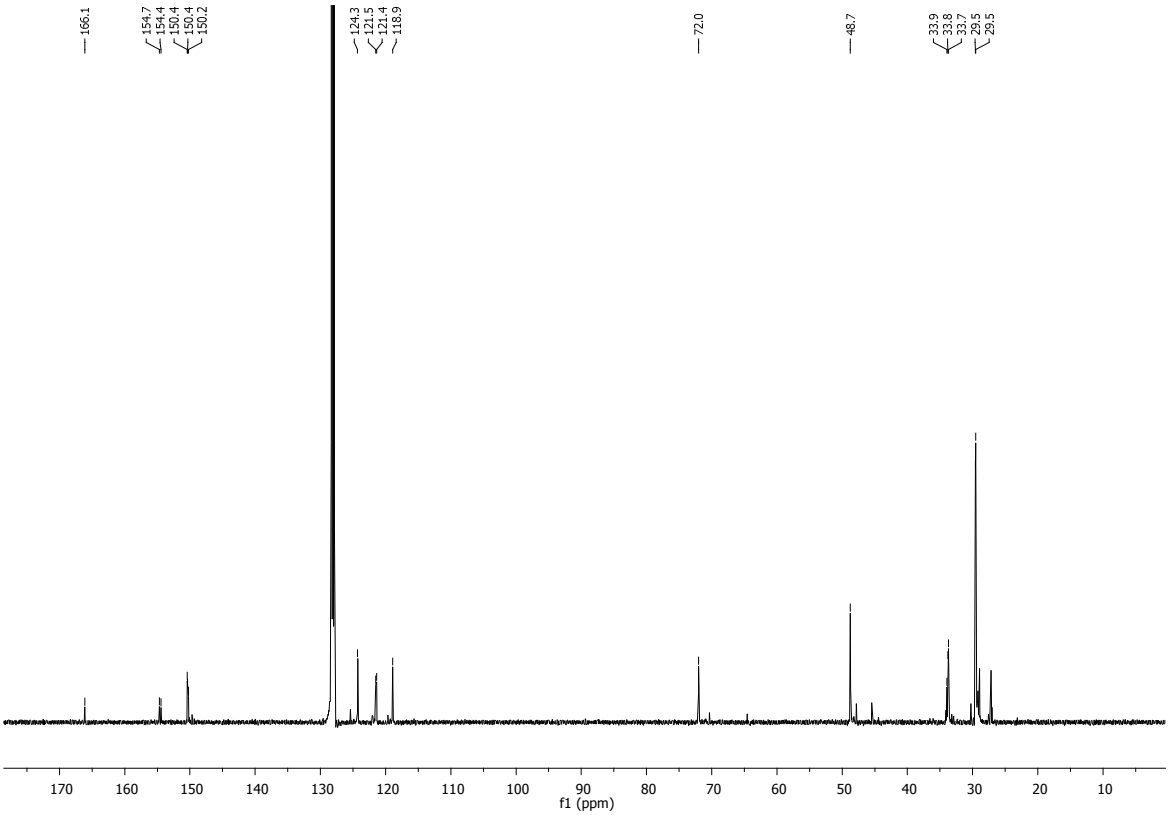

Figure S9. $^{13}C\{^{1}H\}$ NMR spectrum (126 MHz, C_6D_6) of $\{(PCN^{Me})Ni\}_2(\mu\text{-}CO_3)$(**10**)

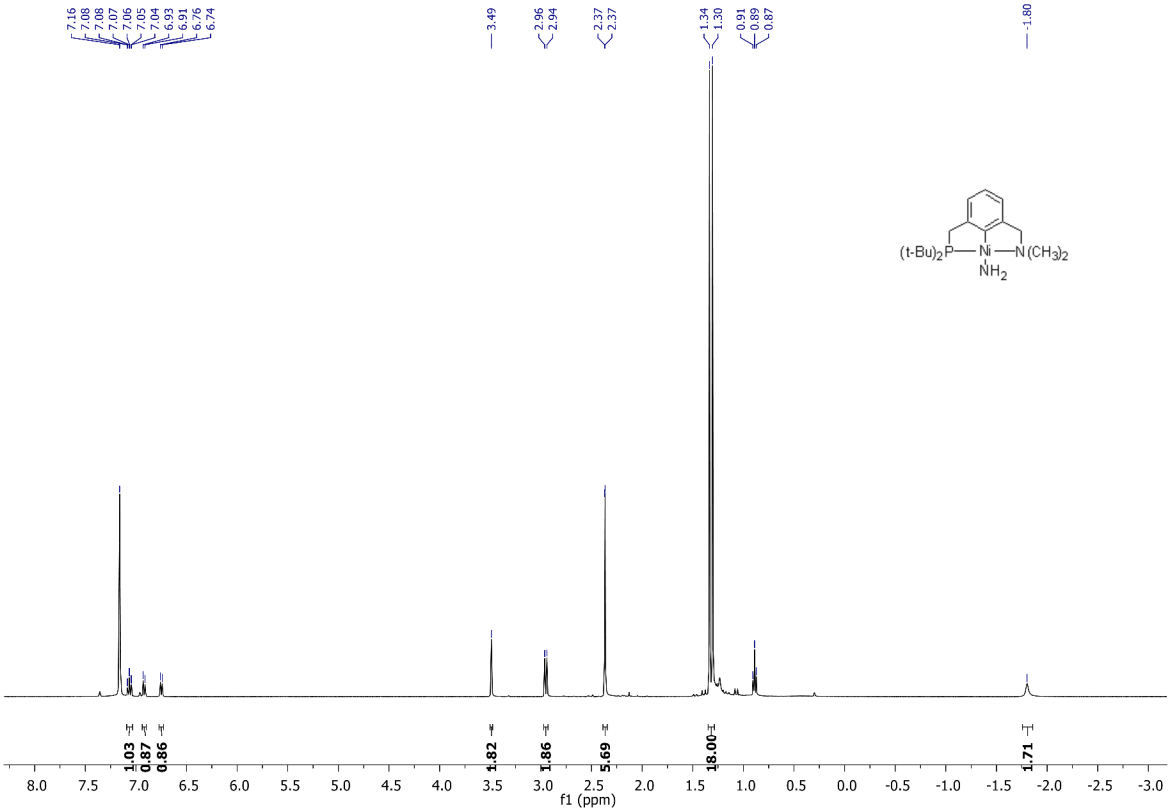

Figure S10.^{1}H NMR spectrum (500 MHz, C_6D_6) of $(PCN^{Me})Ni\text{-}NH_2$(**11**) including traces of hexane and benzene.

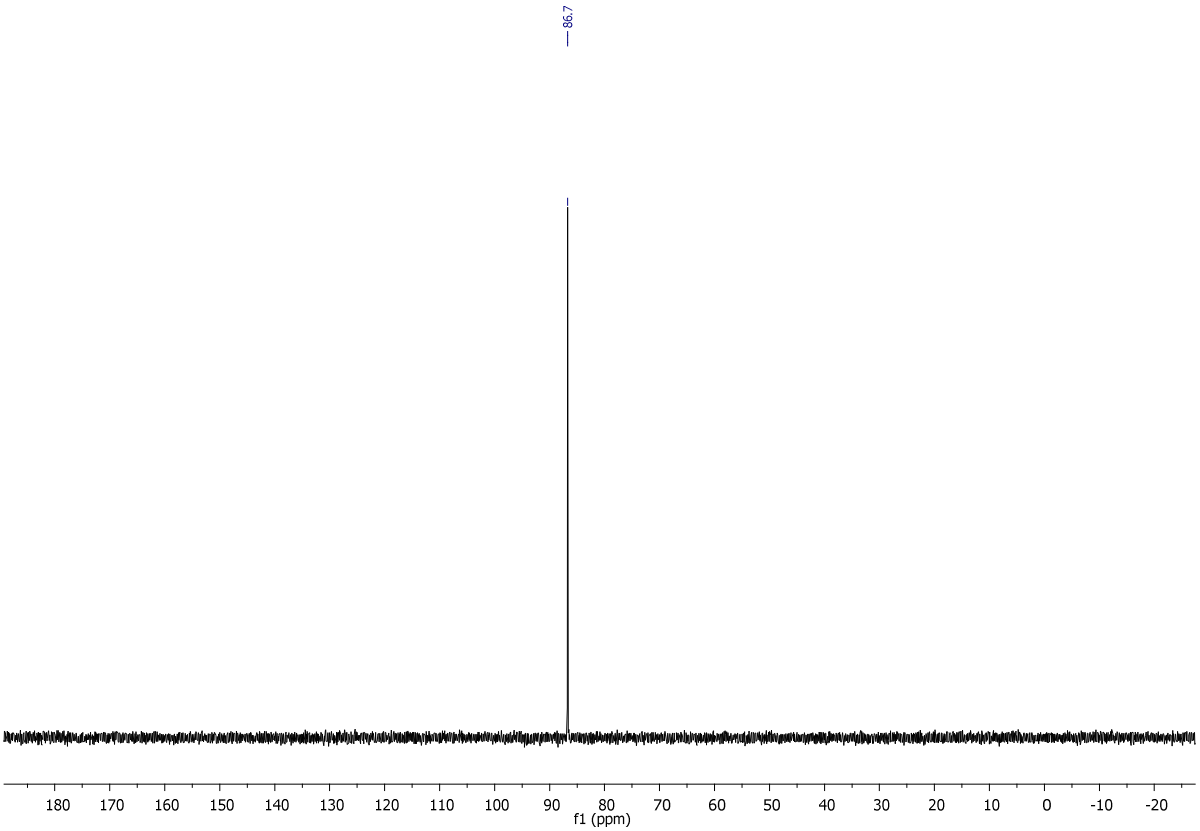

Figure S11.$^{31}P\{^{1}H\}$ NMR spectrum (202 MHz, C_6D_6) of (PCN^{Me})Ni-NH_2(**11**).

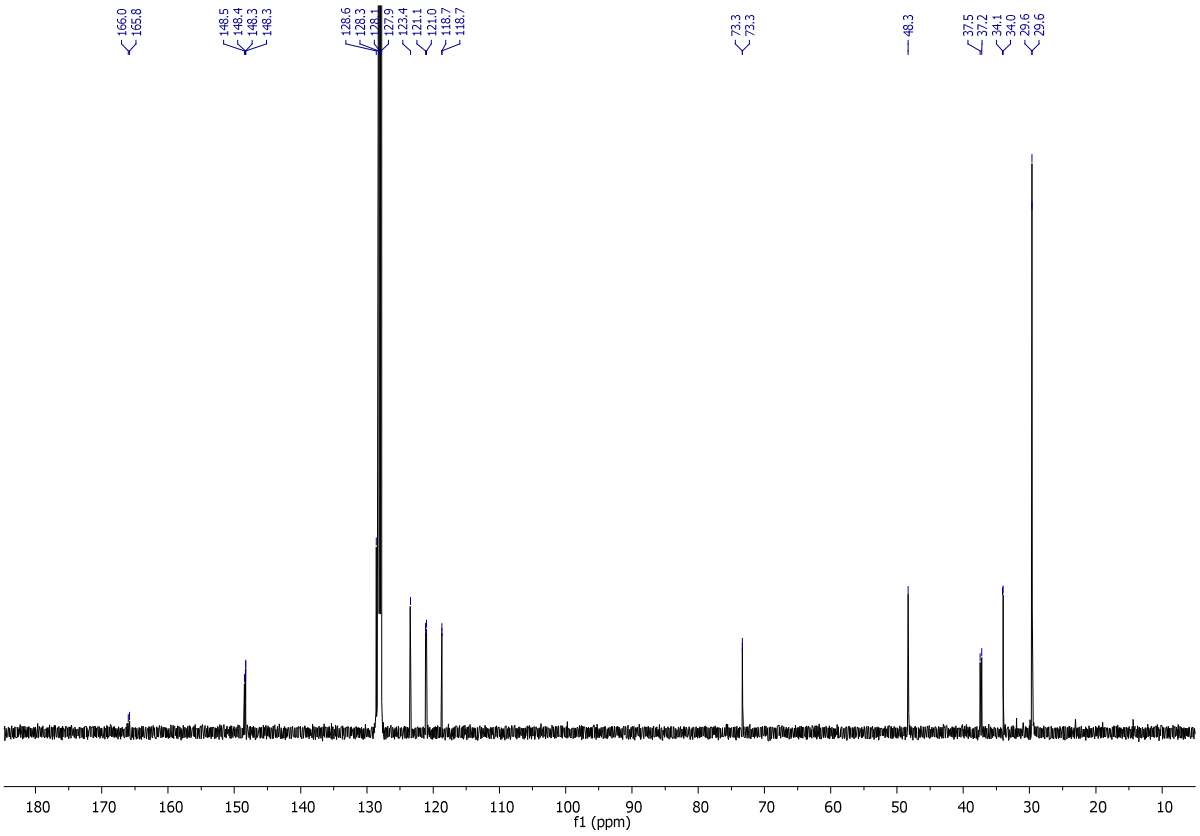

Figure S12. $^{13}C\{^{1}H\}$ NMR spectrum (126 MHz, C_6D_6) of (PCN^{Me})Ni-NH_2(**11**) including traces of hexane and benzene.

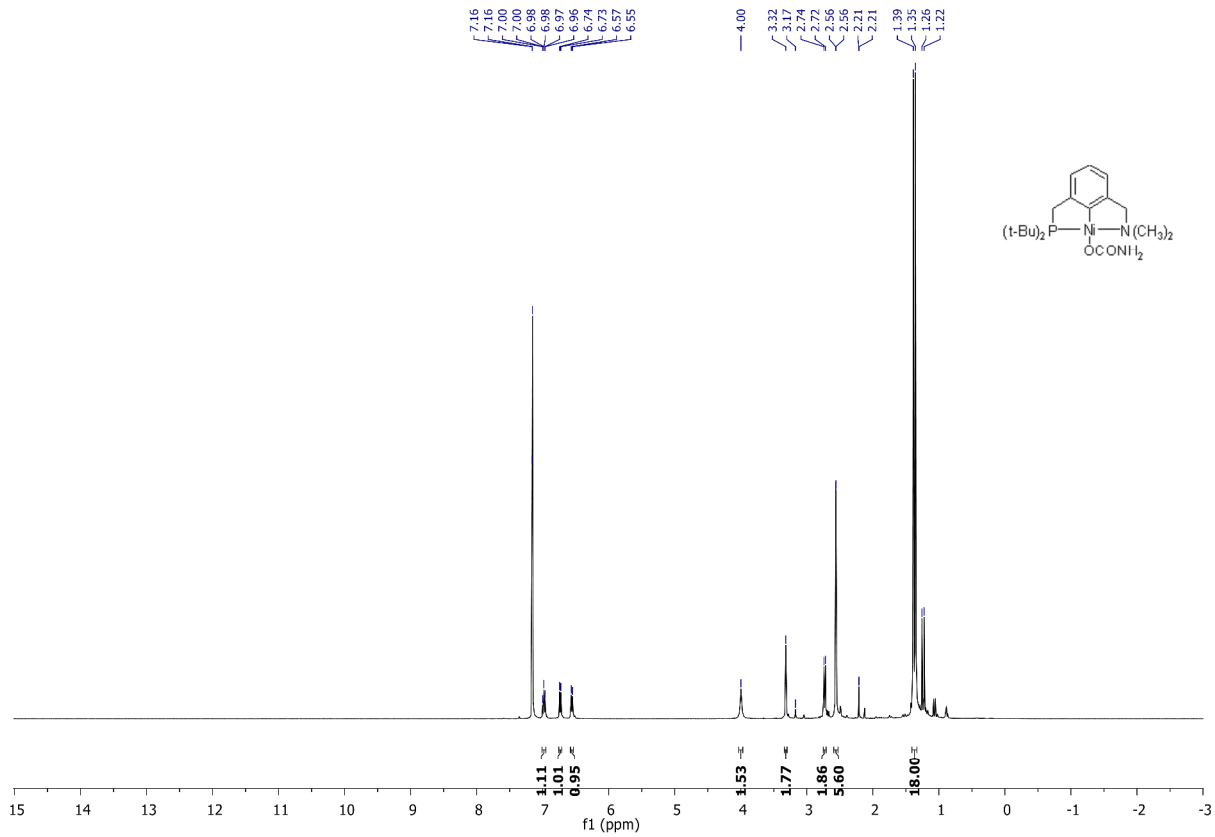

Figure S13.[1]H NMR spectrum (500 MHz, C_6D_6) of (PCN^{Me})Ni-$OCONH_2$(**12**)

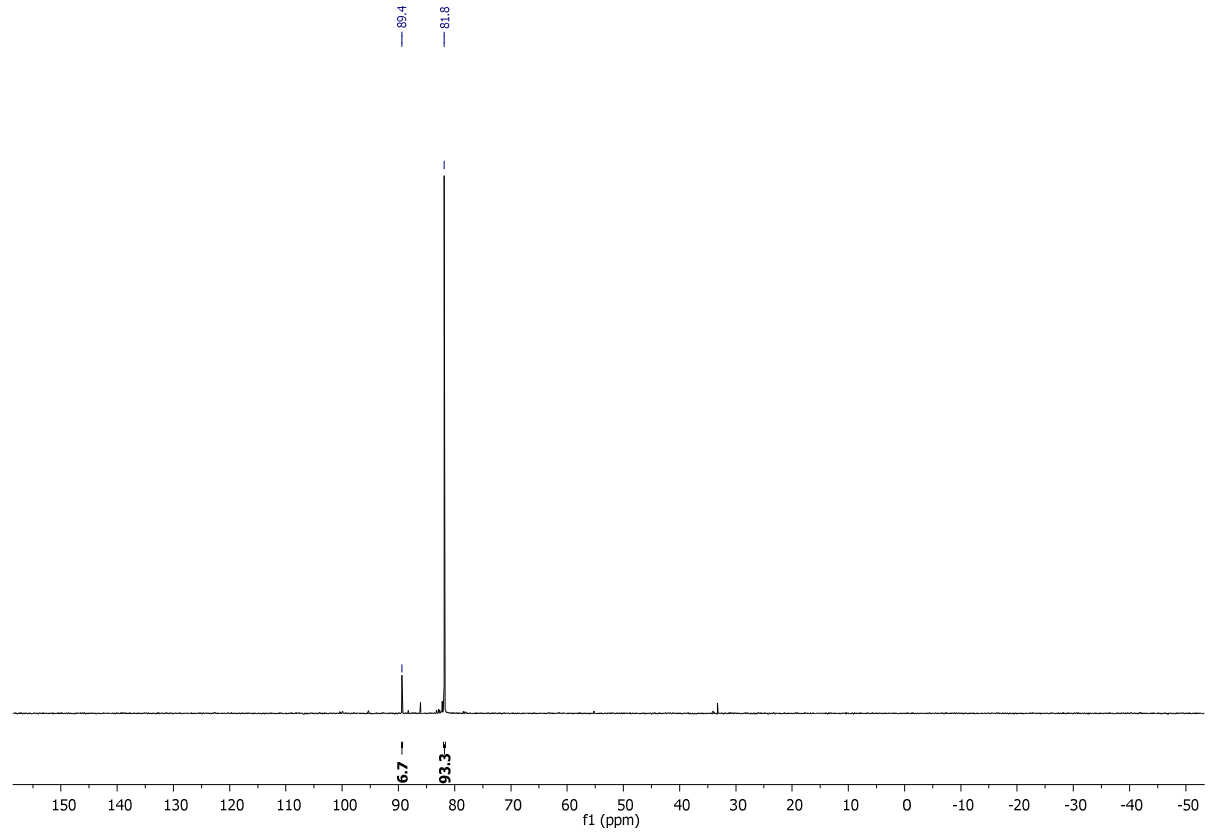

Figure S14.$^{31}P\{^1H\}$ NMR spectrum (202 MHz, C_6D_6) of (PCN^{Me})Ni-$OCONH_2$(**12**).

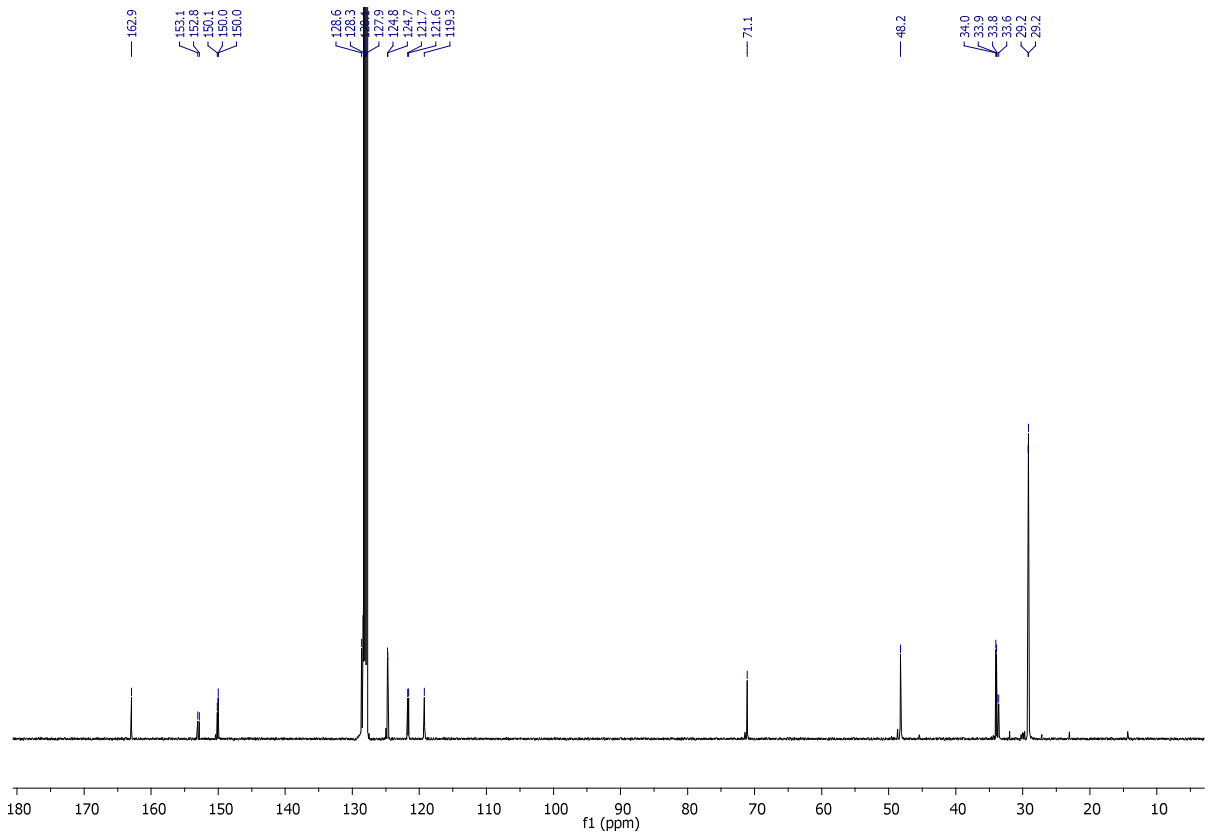

Figure S15.$^{13}C\{^{1}H\}$ NMR spectrum (126 MHz, C_6D_6) of (PCN^{Me})Ni-$OCONH_2$(**12**)

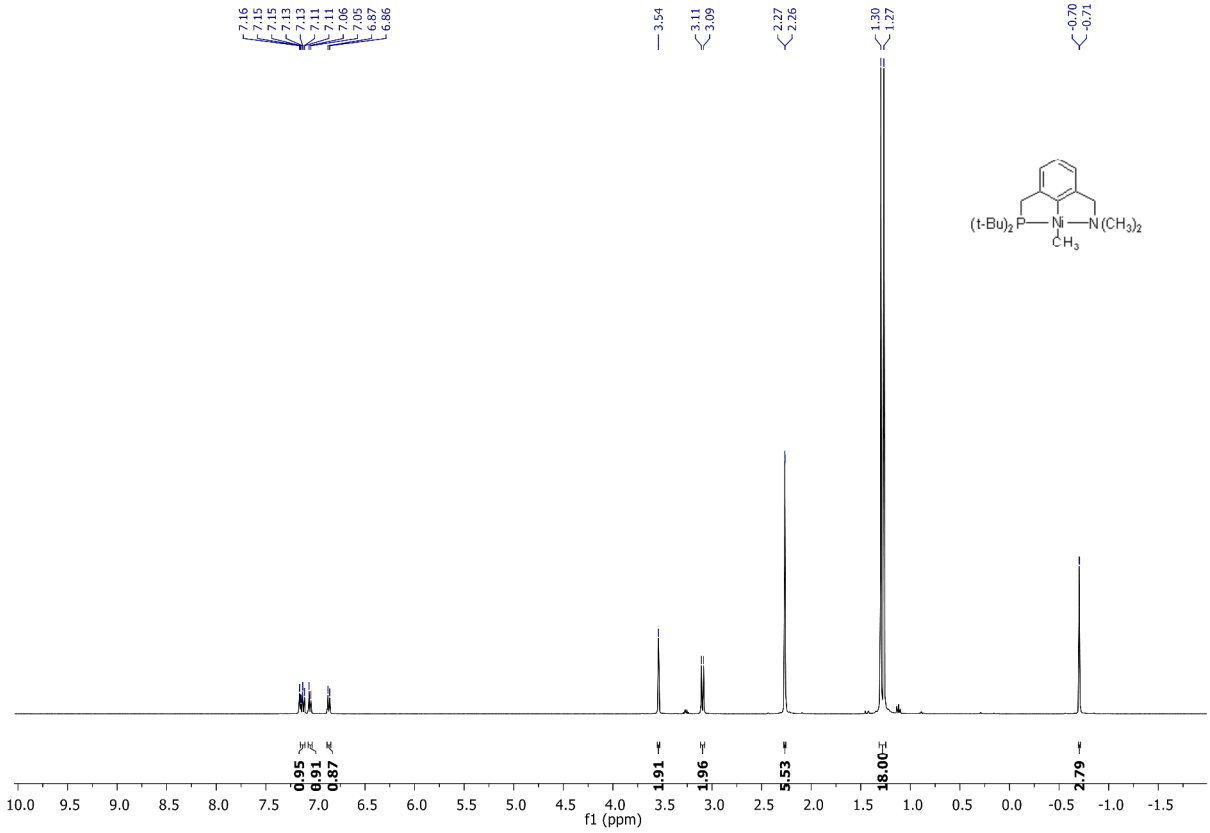

Figure S16.^{1}H NMR spectrum (500 MHz, C_6D_6) of (PCN^{Me})Ni-CH_3(**13**)

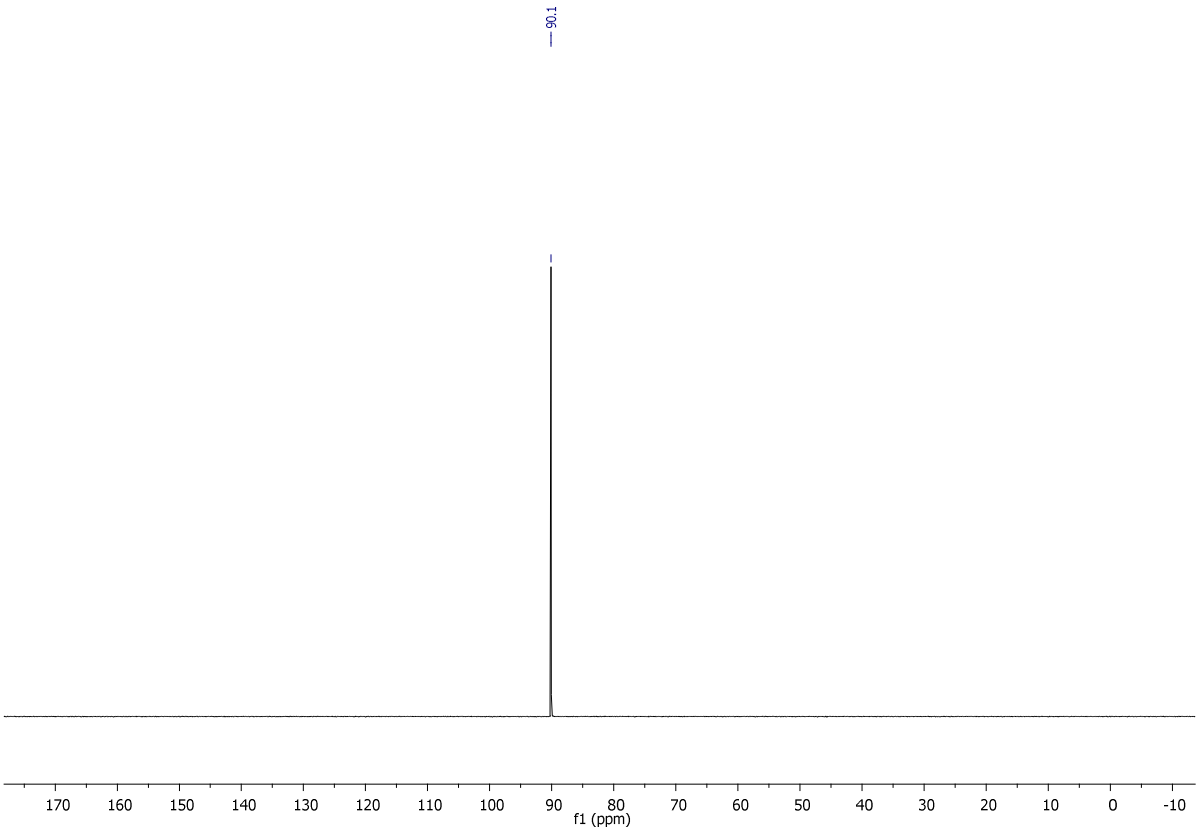

Figure S17.$^{31}P\{^{1}H\}$ NMR spectrum (202 MHz, C_6D_6) of (PCN^{Me})Ni-CH_3(**13**)

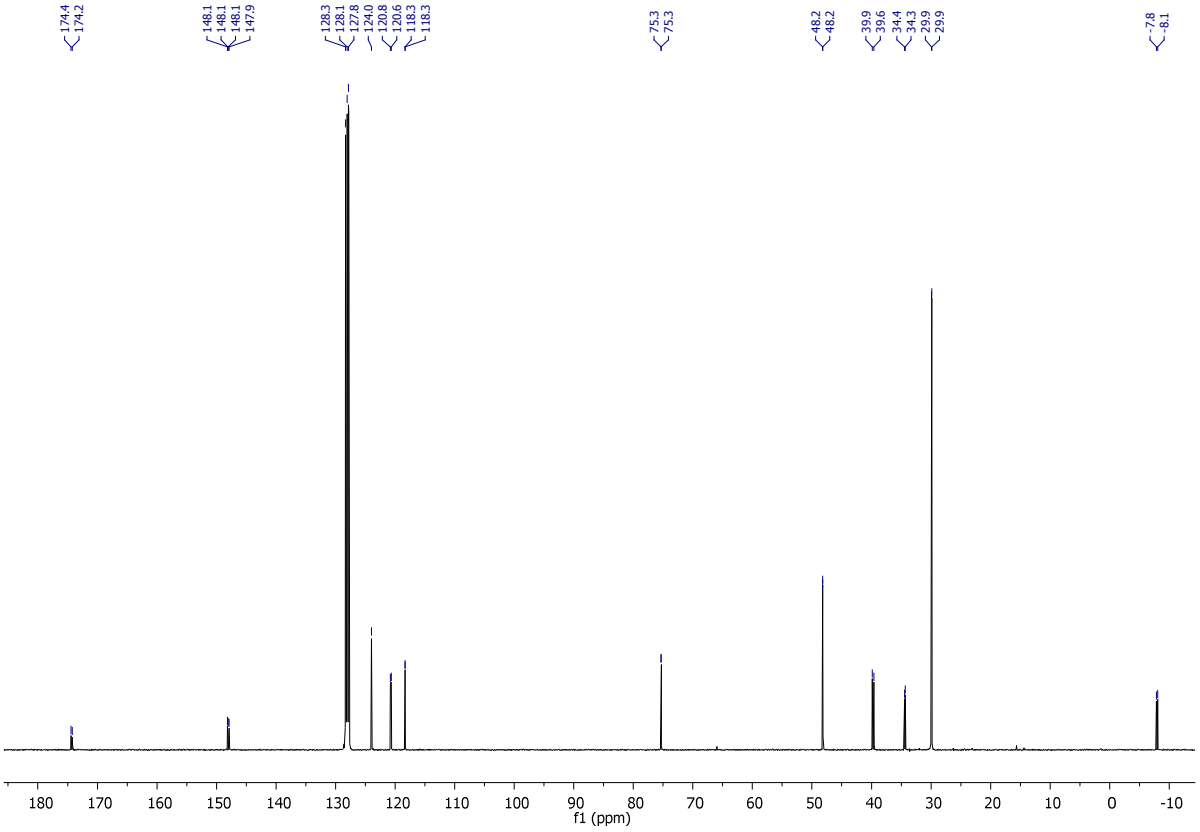

Figure S18.$^{13}C\{^{1}H\}$ NMR spectrum (126 MHz, C_6D_6) of (PCN^{Me})Ni-CH_3(**13**)

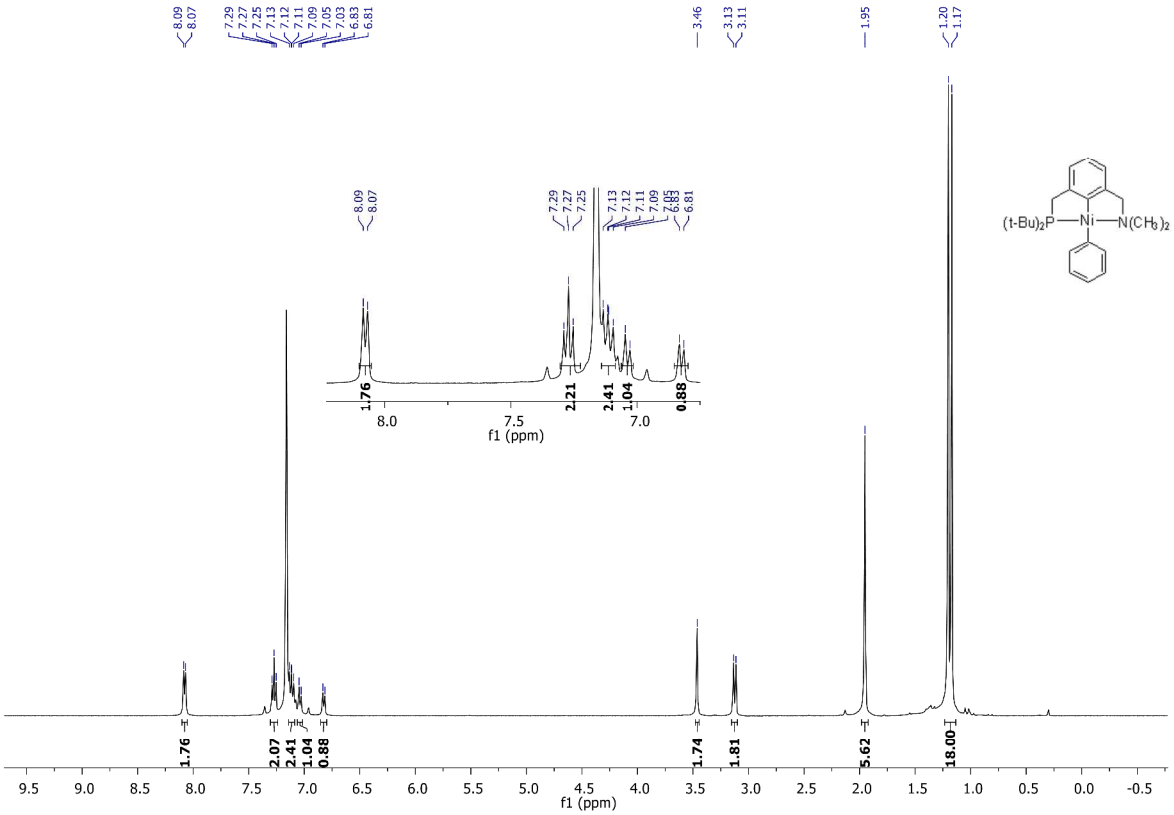

Figure S19.[1]H NMR spectrum (500 MHz, C_6D_6) of the crude (PCN^{Me})Ni-Ph(**14**).

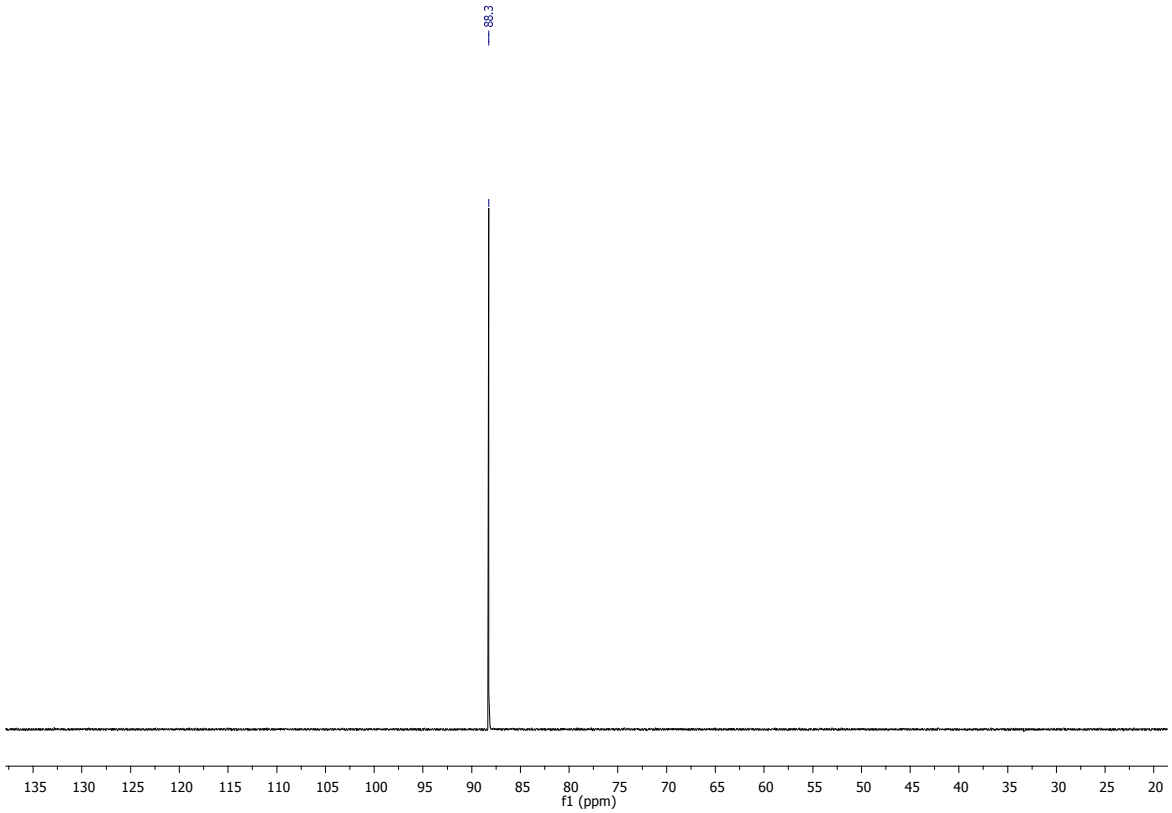

Figure S20. $^{31}P\{^1H\}$ NMR spectrum (202 MHz, C_6D_6) of (PCN^{Me})Ni-Ph(**14**).

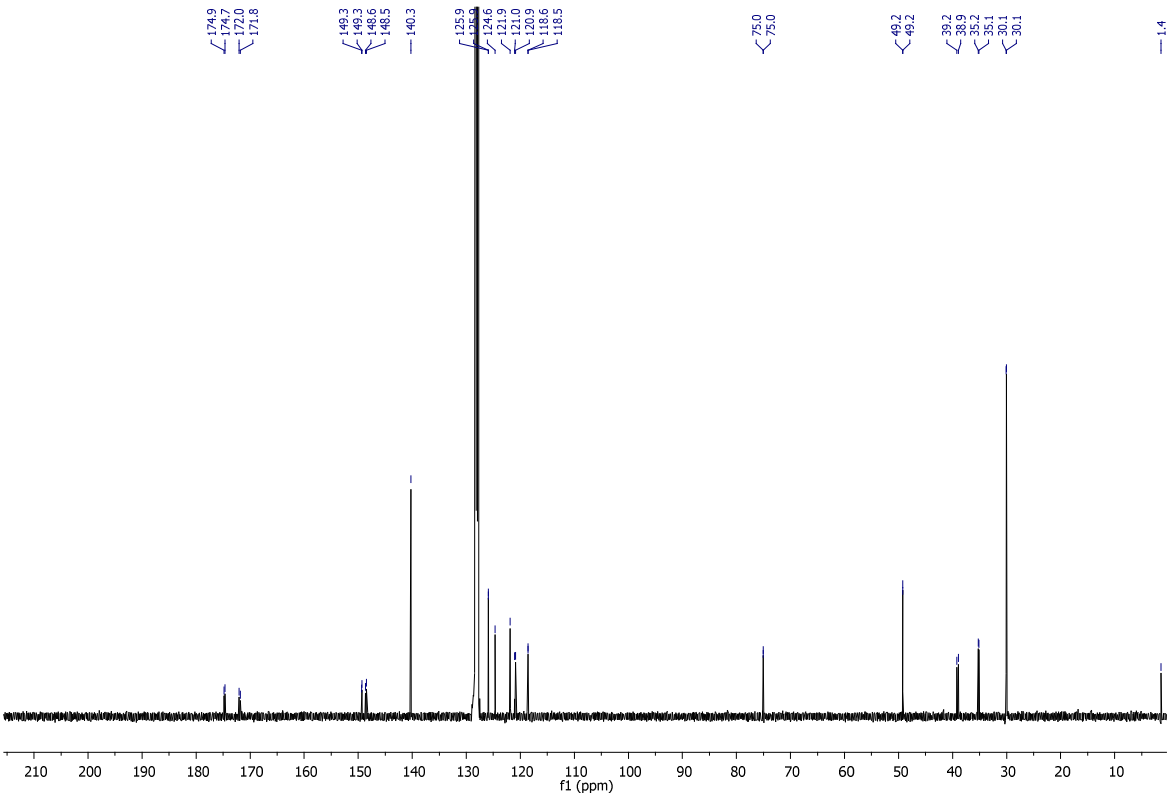

Figure S21.$^{13}C\{^{1}H\}$ NMR spectrum (126 MHz, C_6D_6) of (PCN^{Me})Ni-Ph(**14**)

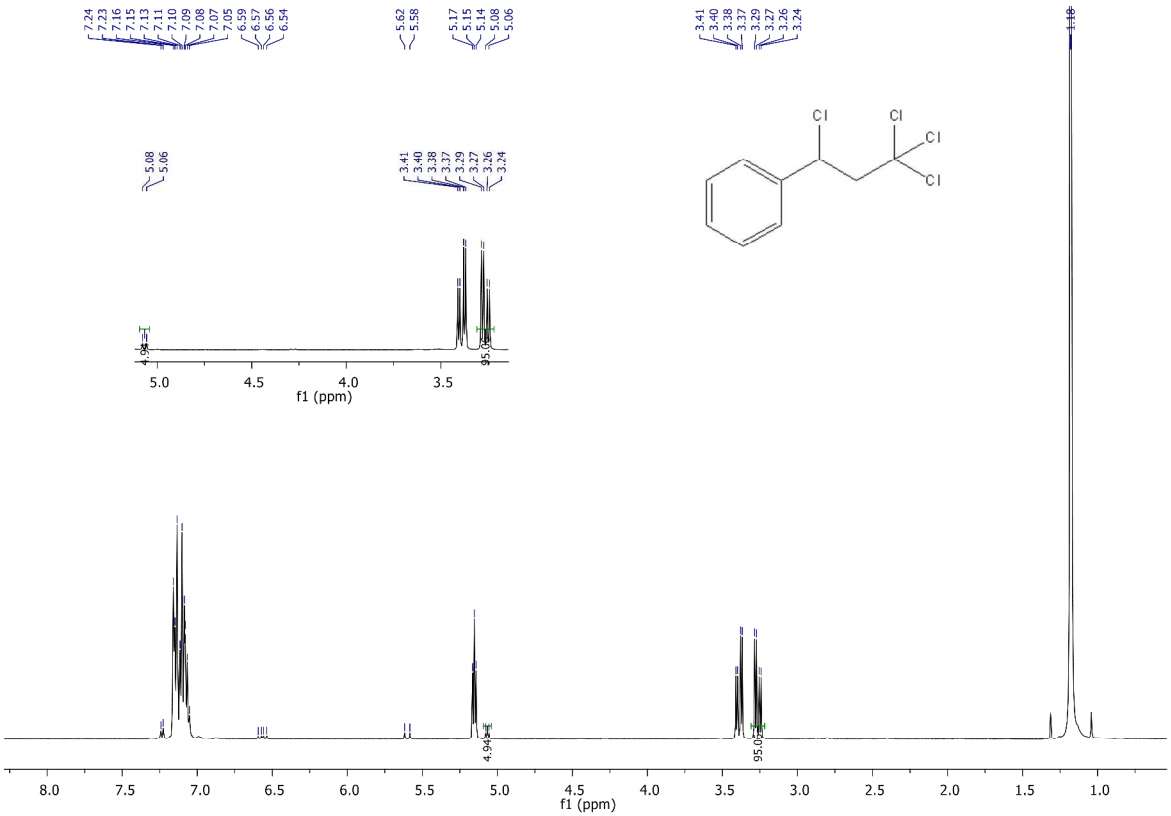

Figure S22.[1]H NMR spectrum (500 MHz, C_6D_6) of in situ Kharasch addition reaction of CCl_4 to styrene after 24h (PCN^{Me})Ni Br(**3**) as a catalyst.

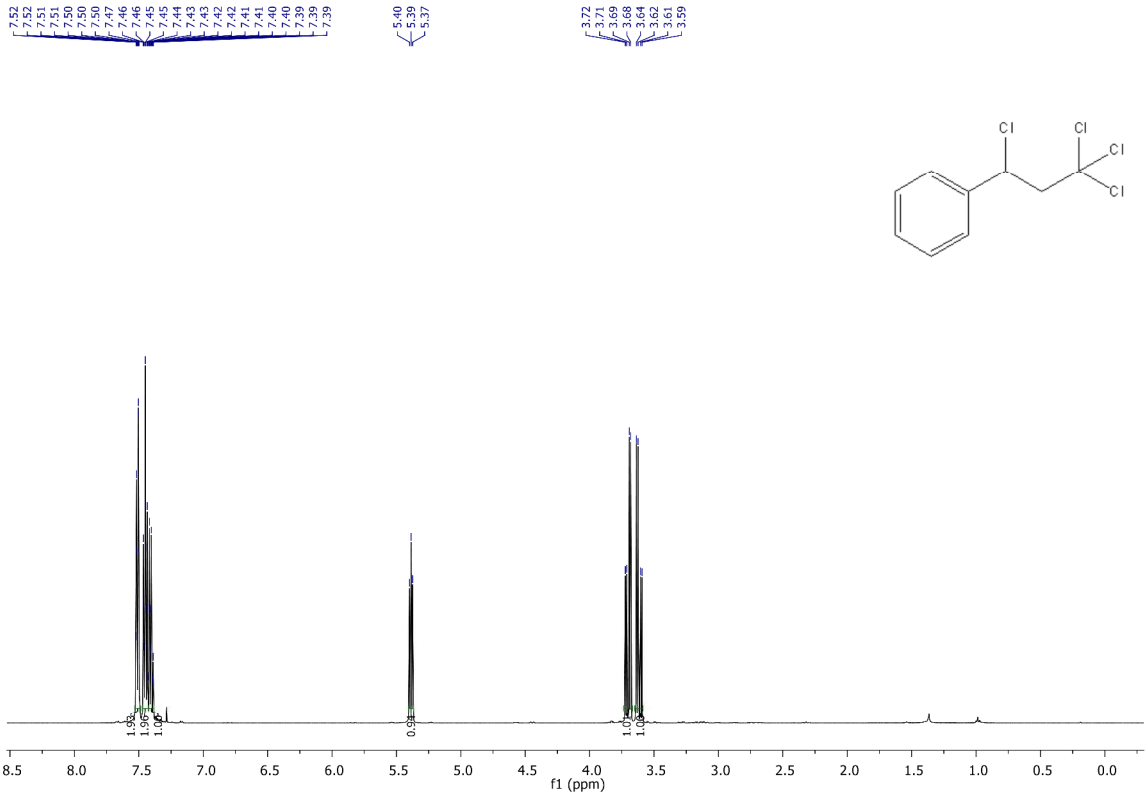

Figure S23.[1]H NMR spectrum (500 MHz, C_6D_6) of (1,3,3,3-Tetrachloropropyl) benzene

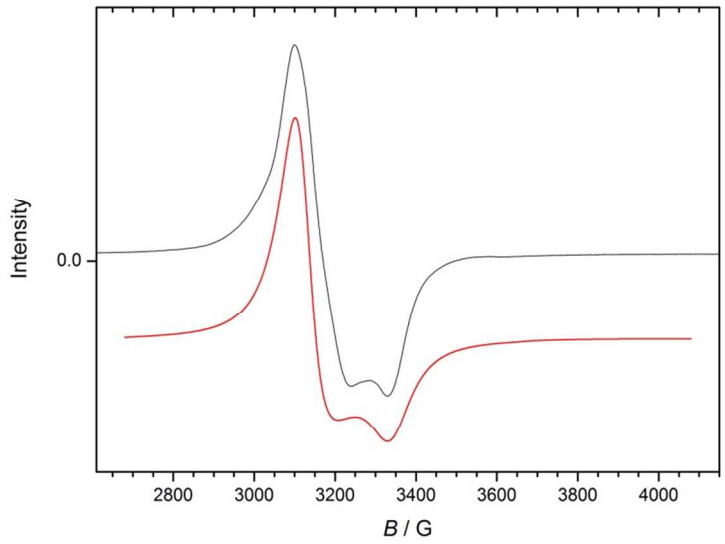

Figure S24. Experimental (black) and simulated (red) X-band EPR spexctra of undiluted **5** in the solid state. The spectrum was recorded at *T*=11K, with *P*= 0.6325 mW; modulation amplitude = 1.0 G, modulation freq. = 100 kHz. Simulation parameters: g_{zz}= 2.065, g_{xx} = g_{yy} = 2.206, lorentzian derivative line shape, FWHH = 65 G.

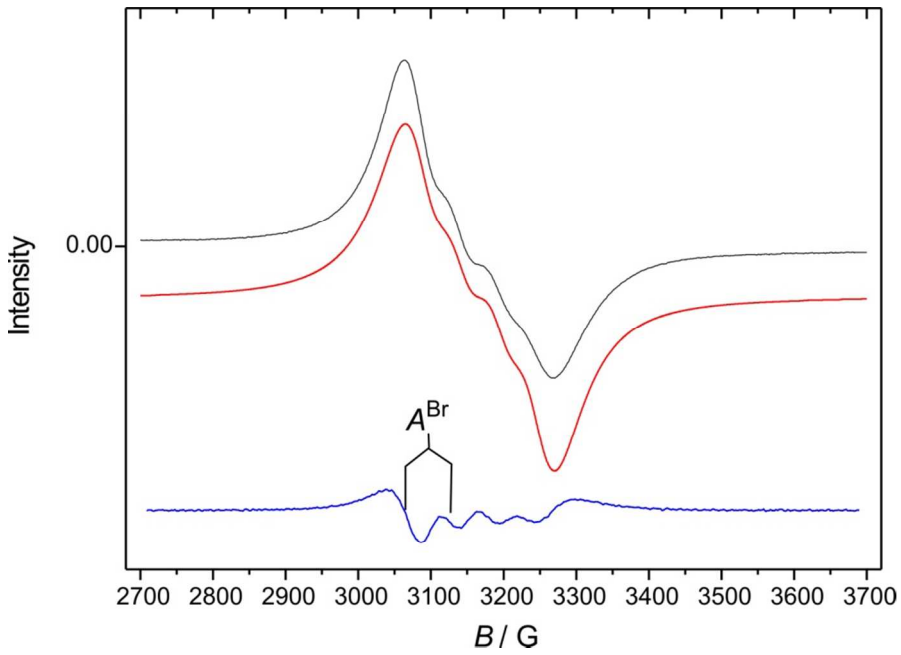

Figure S25. Experimental (black) and simulated (red) X-band EPR spexctra of **5** in a CH_2Cl_2 solution at T=293 K. The blue curve is the derivative of the experimental spectrum directly visualizing the super-hyperfine splitting from coupling to one bromide ligand. The spectrum was recorded with P= 6.325 mW; modulation amplitude = 4.0 G, modulation freq. = 100 kHz. Simulation parameters: g_{iso}= 2.172, $A^{Br}_{iso.}$ = 0.0053 cm^{-1}, lorentzian derivative line shape, FWHH = 63 G.

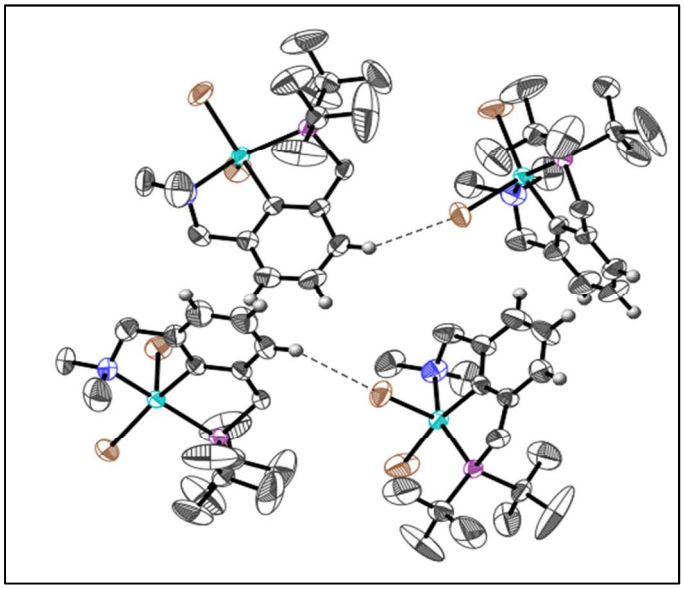

Figure S26. Crystal packing of complex **5** showing a weak non-classical hydrogen bond between the apical bromide ligand and the meta C-H group on an adjacent phenyl ring.